IEEE Access
Multidisciplinary : Rapid Review : Open Access Journal

Received 20 July 2022, accepted 7 August 2022, date of publication 16 August 2022, date of current version 19 August 2022.

Digital Object Identifier 10.1109/ACCESS.2022.3198701

RESEARCH ARTICLE

Rolling Bearing Fault Diagnosis Based on Time-Frequency Feature Extraction and IBA-SVM

MEI ZHANG, JUN YIN, AND WANLI CHEN
College of Electrical and Information Engineering, Anhui University of Science and Technology, Huainan, Anhui 232001, China
Corresponding author: Jun Yin (2296429136@qq.com)

This work was supported in part by the Natural Science Foundation of the Higher Education Institute of Anhui Province under Grant KJ2020A0309, and in part by the National Natural Science Foundation of China under Grant 51874010.

ABSTRACT Accurate fault diagnosis of rolling bearings is necessary to ensure the safe and reliable operation of mechanical equipment. Aiming at the problem of low accuracy of rolling bearing fault diagnosis, a rolling bearing fault diagnosis algorithm based on time-frequency feature extraction and improved bat algorithm-support vector machine (IBA-SVM) model is proposed in this paper. In this algorithm, the feature of the vibration signal in time domain and the frequency spectrum signal obtained by fast Fourier transform (FFT) is extracted, and then the multi-dimensional scaling is used. Multiple dimensional scaling (MDS) algorithm is adopted to reduce the data dimension of eigenvalues to reduce the model complexity, and finally improves the iteration speed and diagnosis accuracy. The improved bat algorithm (IBA) algorithm is used to optimize the parameters of the support vector machine (SVM) model, and the optimal IBA-SVM diagnosis model is obtained for determining the fault type of the rolling bearing. The experimental results show that the accuracy of the proposed rolling bearing fault diagnosis method can reach 99.6667%, which is significantly higher than the state-of-the-art models, and its robustness is stronger. Compared with the existing that use the time-domain or frequency-domain features alone, the proposed algorithm that combines time-domain and frequency-domain features shows significantly improved accuracy in fault diagnosis.

INDEX TERMS Rolling bearing, fault diagnosis, feature extraction, IBA algorithm, SVM model.

I. INTRODUCTION

Rolling bearings are widely used in rotating machinery, and their running state is directly related to the performance of these rotating machinery. So, it is of great significance to conduct the fault diagnosis of rolling bearings [1], [2]. When the bearing surface is damaged, it will produce periodic impact during operation, and its vibration signal will contain abundant fault features. At present, fault diagnosis based on vibration signal is the frontier and hotspot of rolling bearing fault diagnosis [3], [4], [5].

In recent years, with the development of machine learning, Artificial intelligence is associated with the field of fault diagnosis and residual life research, which provides a new method for traditional fault diagnosis [6], [7], [8]. And some intelligent algorithms have been applied to bearing fault diagnosis [9], [10]. The commonly-used algorithms include SVM, back propagation (BP) neural network and extreme learning machine (ELM) [11]. Gao *et al.* proposed an innovative optimized adaptive deep belief network (SADBN) to address the problem of rolling bearing fault identification. The salp swarm algorithm is used to optimize the DBN, which effectively improve the classification accuracy of the DBN [12]. By directly extracting the time-domain component of the bearing vibration signal as the feature vector, Aisong *et al.* used the bat algorithm (BA) to optimize the ELM and overcame the inherent instability of ELM. After the optimization, the average recognition rate reached 99.17%, but there were still some problems such as the difficulty in determining the number of hidden layers of ELM and the

The associate editor coordinating the review of this manuscript and approving it for publication was Baoping Cai.

small test sample size [13]. Liye *et al.* proposed a method of feature extraction based on the improved empirical mode decomposition (EMD), and then used generalized state space averaging to extract the features of SVM [14]. But there are still some problems such as prematurity and low selection accuracy. Qian *et al.* proposed the sparrow search algorithm to optimize the machine learning method of ELM to classify and diagnose the rolling bearing faults of motor. Realize the classification and diagnosis of rolling bearing faults more quickly, which proves the time-based stability of the proposed model [15]. Xiaoting *et al.* proposed a method of using Hanning window to window the frequency-domain signal to obtain the root mean square eigenvalue of the sample features, and they used the SVM optimized by Cuckoo Algorithm (CS-SVM) to classify the samples [16]. Window processing can effectively select sample length, but the characteristic values selected by the diagnosis model lack of comprehensiveness, which speeds up the computing speed to a certain extent, but also leads to unsatisfactory diagnosis effect. Qiang and Wenlong used wavelet packet analysis to extract bearing fault features, and adopted chaotic dynamic weight and particle swarm optimization (PSO) to optimize BP neural network for rolling bearing fault diagnosis. However, the model selection and optimization of this method are not novel enough, and it does not achieve better diagnosis effect in the field of bearing faults. Feng *et al.* proposed an improved quantum bee colony optimization algorithm In these two papers, bearing fault diagnosis is connected with neural network And satisfying results have been achieved [17], [18], [19].

SVM is a machine learning algorithm for classification, which is widely used in pattern recognition, portrait recognition, data analysis and text classification.

SVM also plays an important role in the field of fault diagnosis. In transformer fault diagnosis, the most commonly used fault diagnosis method is Dissolved Gas Analysis in oil (DGA), because the cause and type of power transformer fault cannot be directly measured. Power transformer in overheating, discharge and other states, the insulation oil will produce gas, and dissolved in the oil. Then the intelligent algorithm is used to analyze the dissolved gas to get the running status of the transformer. SVM and other intelligent algorithms for fault diagnosis can deal with the lack of expert experience and difficult to accurately judge the power transformer fault type; However, its DGA data varies greatly, and it has poor classification effect on the data near the threshold value. It often appears the phenomenon of "missing code" or "overcode," and cannot adapt to the fault diagnosis in large-scale power grid [20].

In the asynchronous motor fault diagnosis, SVM can be directly input from the original data or denoised data, the model structure is simple, and avoids the shortcomings of asynchronous motor modeling inaccurate in the analytical method. However, in the face of unknown complex interference, SVM cannot carry out effective feature mining, and the recognition effect can only meet some significantly different event signals, but not meet the recognition of various unknown interference.

The rolling bearing vibration signal mechanism is complex, with non-smooth and non-Gaussian characteristics. In terms of data acquisition, the ratio of healthy data to faulty data is seriously unbalanced because the equipment is in good health in most cases and is only in a faulty state in very few cases. In addition, in the real environment, the collected data will be mixed with various kinds of noise in addition to the vibration of the measured bearing. Therefore, in order to achieve good diagnostic effect, the fault diagnosis model is required to be suitable for limited samples and has certain noise immunity, SVM model has strong superiority in analyzing and dealing with non-smoothness and non-linearity, and has strong generalization ability, which can well solve small sample data set and non-linearity problem, and has unique advantages and good application prospect in rolling bearing fault diagnosis.

Compared with the traditional BPNN and RF classification models, this model has the advantages of simplicity, practicability and excellent classification effect. In addition, SVM has been applied in the field of bearing fault diagnosis, which has verified its excellent classification effect in many aspects. Therefore, SVM is chosen as the basic fault diagnosis model in this paper. The core parameters in the SVM model are C and G, where C is a penalty coefficient representing the tolerance to error, and G is a parameter of the function itself when the kernel function is selected as the radial basis function, which affects the speed of training and prediction. If the default parameters of the model are used, the overfitting or underfitting phenomenon easily occurs; if the parameters are adjusted manually, the workload is large, and it is not easy to find the optimal parameters. Therefore, it is necessary to select the appropriate optimization algorithm to optimize the relevant parameters.

BA is a population-based stochastic optimization algorithm proposed by Yang, a scholar of Cambridge University, in 2010 by simulating the echolocation behavior of bats, which has strong search ability. BA, which simulates this foraging mode, provides a completely different scheme to solve the problems of poor local search performance and low convergence accuracy [21]. The IBA improves the optimization formula on the basis of the traditional BA, and has stronger ability to search for the optimal parameters, which is suitable for the parameter optimization of the classification diagnosis model. Bat algorithm is a swarm intelligence optimization algorithm based on iterative optimization technology, which initializes a group of random solutions, then iteratively searches for the optimal solution, and generates local new solutions by random flight around the optimal solution to enhance the local search speed. It has the advantages of simple model, fast convergence speed and few parameters, and has been applied in engineering optimization, model recognition and fault diagnosis. BA is used as the basic optimization algorithm to optimize the classifier in [22] and [23], achieved good results in the field of bearing diagnosis. It is proved that the optimization effect and adaptability of BA for SVM classifier still occupy a certain position in many swarm intelligence algorithms, so it is appropriate to select BA as the optimization algorithm.

Therefore, this paper proposes a rolling bearing fault diagnosis algorithm based on time-frequency feature extraction and IBA-SVM model. The algorithm integrates the time-domain and frequency-domain features of rolling bearing vibration signals for feature extraction, and then establishes the SVM model optimized by IBA algorithm. The training and testing of the model is carried out. Finally, the accurate diagnosis of rolling bearing fault is realized.

The paper is organized as follows: Section 1 introduces the current research status of rolling bearing fault diagnosis and its related algorithms by domestic and foreign researchers; Section 2 introduces the principles of the related algorithms used in this paper, including algorithms used in data preprocessing, SVM model and IBA algorithm; Section 3 introduces the rolling bearing fault diagnosis model established in this paper; Section 4 presents an example analysis using the fault diagnosis model proposed in this paper to verify the feasibility and superiority of the model; Section 5 summarizes the whole paper, and reflections on existing diagnostic methods and perspectives on future research directions.

II. BASIC THEORY PART

In view of the signal characteristics of rolling bearings mentioned above, the fault diagnosis model must have good practical application and robustness to adapt to the complex and changeable fault vibration signals. Therefore, the selection of appropriate algorithm and model is one of the factors that must be considered in bearing fault diagnosis.

A. FAST FOURIER TRANSFORM (FFT)

FFT is an engineering realization method of discrete Fourier Transform (DFT). According to the properties of rotation factor in DFT solution and the divide-and-conquer idea, the calculation process is simplified.

The DFT formula is as follows:

$$X(k) = \sum_{n=0}^{N-1} x(n) e^{-j(2\pi/N)kn}, 0 \leq k \leq N-1 \tag{1}$$

where $X(k)$ is a frequency spectrum function of a bearing vibration signal, $x(n)$ is a discrete signal representing the vibration of the bearing in time domain, and N is the sample length.

Multiply N^2 complex numbers with $N(N-1)$ complex number addition:

$$X(k) = \sum_{n=0}^{N-1} x(n) \omega_N^{kn} \tag{2}$$

where ω is the rotation factor to be replaced: $\omega_N^{kn} = e^{-jk\frac{2\pi}{N}n}$ and $\omega = e^{-j\frac{2\pi}{N}}$

The time-domain signal $x(n), n = 1, 2, \ldots, N-1$, t divided into two parts according to the index:

$$\begin{cases} f_{even}(n) = x(2n) \\ f_{odd}(n) = x(2n+1) \end{cases} \tag{3}$$

At this point, the index range is: $n = 0, 1, \ldots, \frac{N}{2} - 1$. After simplification of Eq. (2), it can be obtained:

$$\begin{aligned} x(k) = &\sum_{n=even} x(n)\omega_N^{kn} \\ &+ \sum_{n=odd} x(n)\omega_N^{kn}, n = 0, 1, \ldots, N-1 \end{aligned} \tag{4}$$

According to the scaling of the rotation factor, further conversion:

$$x(k) = \sum_{m=0}^{(N/2)-1} f_{even}(m)\omega_{\frac{N}{2}}^{k.m} + \omega_N^k \sum_{m=0}^{(N/2)-1} f_{odd}(m)\omega_{\frac{N}{2}}^{k.m} \tag{5}$$

That is:

$$x(k) = F_{even}(k) + \omega_N^k F_{odd}(k), k = 0, 1, \ldots, N-1 \tag{6}$$

where $F_{even}(k)$ is the result of even index input $f_{even}(n)$, $F_{odd}(k)$ is the result of odd index input $f_{odd}(n)$.

B. MULTIPLE DIMENSIONAL SCALING (MDS)

MDS solves the problem: when the similarity between N objects is given, determine the representation of these objects in the low-dimensional space, and make it roughly match the original similarity as far as possible. Each point in a high-dimensional space represents an object, so the distance between points is highly correlated with the similarity between objects.

For n instances, each instance is a vector of dimension $(1 \times m)$. The distance matrix D in m-dimensional space is a $(N \times N)$ matrix. The element d_{ij} in D represents the distance between the i th point and the j th point.

Now the original data is mapped to the Z-dimensional space, and the distance between any two points is required to be the same as that in the original space. Therefore:

$$d_{ij}^2 = ||Z_i - Z_j||^2 = ||Z_i||^2 + ||Z_j||^2 - 2Z_i^T Z_j \tag{7}$$

Without loss of generality, it is assumed that all points in Z-dimensional space are centralized, namely:

$$\sum_{i=1}^{N} Z_i = 0 \tag{8}$$

Sum both sides of Eq. (7):

$$\begin{cases} \sum_{i=1}^{N} d_{ij}^2 = \sum_{i=1}^{N} ||Z_i||^2 + N||Z_j||^2 \\ \sum_{j=1}^{N} d_{ij}^2 = \sum_{j=1}^{N} ||Z_j||^2 + N||Z_i||^2 \end{cases} \tag{9}$$

Sum over Eq. (7) again:

$$\sum_{i=1}^{N} \sum_{j=1}^{N} d_{ij}^2 = 2N \sum_{i=1}^{N} ||Z_i||^2 \tag{10}$$

The inner product matrix $B = Z^T Z$ was defined, and the eigenvalue decomposition was performed to obtain the eigenmatrix:

$$B = V \Lambda V^T \tag{11}$$

where Λ is the eigenvalue matrix, and V is the eigenvector matrix.

In Z-dimensional space, the first Z largest eigenvalues and eigenvectors are selected. The data points after dimensionality reduction are expressed as:

$$Z = V_Z \Lambda_Z^{\frac{1}{2}} \tag{12}$$

C. SVM

The core of SVM algorithm is to find the boundary plane with the best classification effect, which ensures the classification effect while the interval distance is also optimal.

Let the training set for the binary classification problem be:

$$Data = \{(x_i, y_i), x_i \in R^n, y_i \in \{-1, +1\}\}_{i=1}^n \tag{13}$$

where x_i is the first i input data, y_i is the class label corresponding to x_i, and n is the number of training samples.

Let the hyperplane be:

$$f(x) = \omega^T x + b = 0 \tag{14}$$

where ω is a vector perpendicular to a plane, characterizing the direction of the plane, and b is the distance from the origin to the hyperplane.

In order for the hyperplane to properly separate the two types of data samples, it should satisfy:

$$y_i[\omega^T x + b] \geq 1 \tag{15}$$

No matter what the point is, the distance from (x_i, y_i) to the hyperplane is:

$$d = \frac{|\omega^T x + b|}{||\omega||} \tag{16}$$

where $\|\omega\|$ denotes the second order norm of the normal vector ω.

If $\exists \tau > 0$, such that:

$$\frac{y_i f(x)}{||\omega||} \geq \tau \tag{17}$$

The training set Data is said to be linearly separable.

The steps for solving the linear separable SVM are as follows:

Step 1. Minimization problem

$$\min_{\omega,b} \frac{1}{2}\omega^T \omega \tag{18}$$

The constraints are:

$$y_i[\omega^T x + b] \geq 1 \tag{19}$$

Step 2. Build *lagrange* Function

$$L(\omega, b, \lambda) = \frac{1}{2}\omega^T \omega + \sum_{i=1}^{n} \lambda_i [1 - y_i(\omega^T x_i + b)] \tag{20}$$

where λ_i represents *lagrange* multiplier, and $\lambda_i \geq 0$, $i = 1, 2 \ldots n$.

Step 3. Transform into *lagrange* dual problem

$$\max_{\lambda} \min_{\omega,b} L(\omega, b, \lambda) \tag{21}$$

The original quadratic programming problem is transformed into:

$$\max_{\lambda} L(\lambda) = \sum_{i=1}^{n} \lambda_i - \frac{1}{2}\sum_{i=1}^{n}\sum_{j=1}^{n} \lambda_i \lambda_j y_i y_j x_i^T x_j \tag{22}$$

Step 4. Solve the parameters ω^* and b^*

By the Kuhn-Tucker condition:

$$\omega - \sum_{i=1}^{n} \lambda_i y_i x_i = 0 \tag{23}$$

$$\sum_{i=1}^{n} \lambda_i y_i = 0 \tag{24}$$

Then the weight parameter vector of the optimal interface ω and a threshold value b are:

$$\omega = \sum_{i=1}^{n} \lambda_i y_i x_i \tag{25}$$

$$b = -\frac{1}{2}[\omega^T * x(+1) + \omega^T * x(-1)] \tag{26}$$

where $x(+1)$ and $x(-1)$ denote a certain support vector belonging to $y = +1$ and $y = -1$ respectively.

Step 5. The maximum hyperplane is constructed.

$$\omega^T x + b = 0 \tag{27}$$

$$f(x) = sign(\omega^T x + b) \tag{28}$$

where ω and b form an optimal classification plane which can realize the optimal classification of the sample set; and sign is a sign function used for forming a decision function of the sample set to realize the classification prediction of the samples set.

For the sample data that is not linearly separable, it is necessary to introduce it into a high-dimensional space so that the data is linearly separable in this space [24], [25].

D. IBA ALGORITHM

1) BAT ALGORITHM

The individual bat is the basic unit of bat algorithm. In the BA, each virtual bat has a random flight speed at its own position, and the bats have different frequencies, amplitude, and pulse emission rates. When finding prey, the bats will change the frequency, amplitude, and pulse emission rate. Thus, the direction, speed, and distance of the prey are obtained [26], [27], [28].

The optimization process of the BA is as follows:

Step 1. Parameter initialization

Initialize bat population number n, bat location $x_i (i = 1, 2 \ldots n)$, velocity v_i, sound wave frequency f_i, sound wave amplitude A_i and frequency R_i.

Step 2. Find the current best bat position x^* and update the velocity and position

The formula for updating velocity and position is as follows:

$$f_i = f_{\min} + (f_{\max} - f_{\min})\beta \tag{29}$$

$$v_i^{t+1} = v_i^t + (x_i^{t+1} - x^*)f_i \tag{30}$$

$$x_i^{t+1} = x_i^t + v_i^{t+1} \tag{31}$$

where $\beta \in [0, 1]$, which is a random vector, x^* is the current optimal position of the bat in the group, $f_{\min}$ and $f_{\max}$ denote the upper and lower bounds of the frequency, respectively.

Step 3. Generate a local solution near the optimal bat

Randomly generate a number $rand_1$ If $rand_1 > R_i$, then a local solution is generated near the optimal bat:

$$x_{new} = x_{old} + \varepsilon A^t \tag{32}$$

where $\varepsilon \in [-1, 1]$ is a random number, A^t is the average amplitude of the same generation in this bat population.

Step 4. Update bat location and adjust sound wave amplitude and frequency

Randomly generate another number $rand_2$. If $rand_2 < A_i$, and $f(x_{new}) > f(x_{old})$, replace the old bat with a new one and adjust the sound wave amplitude according to:

$$A_i^{t+1} = \alpha A_i^t \tag{33}$$

$$R_i^{t+1} = R_i^0[1 - \exp(-\gamma t)] \tag{34}$$

where $\alpha \in (0, 1)$ represents the acoustic amplitude attenuation coefficient, $\gamma > 0$ represents the pulse frequency enhancement factor, R_i^0 denotes the initial acoustic frequency of the ith bat.

Step 5. Determine whether the maximum number of iterations is reached and output the optimal parameters

If the end condition is not satisfied, return to Step 2, repeat the process, and finally output the optimal parameters to establish the optimal classifier model.

2) IBA ALGORITHM

The traditional BA easily falls into local convergence and lacks global search ability when solving global optimization problems. In order to simulate the predatory behavior of bats more realistically and replace the velocity and position update mode of the original algorithm, the Levy flight mechanism is applied to the BA to enhance the global search ability of the algorithm [29].

The basic Levy flight mechanism still has shortcomings. For example, when the step size factor α is large, although the global search ability is enhanced, the solution accuracy is not high. If the α value is small, the algorithm needs to increase the number of iterations to find the theoretical optimal value of the algorithm, which reduces the efficiency of the algorithm. In view of the above problems, this paper proposes to use the enhanced search Levy flight mechanism to optimize the traditional BA [30]. Step size α is changed

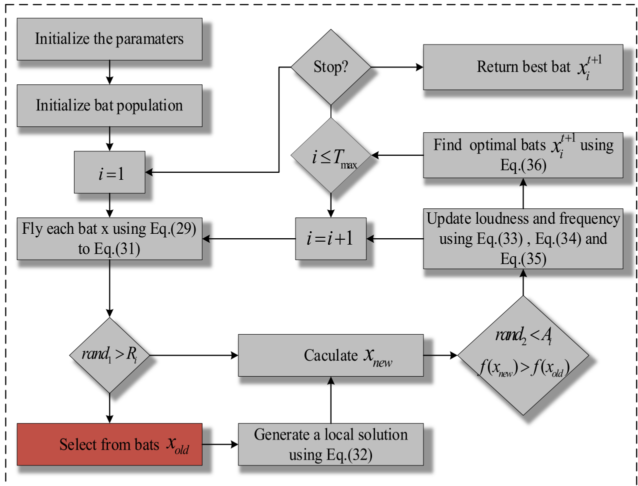

FIGURE 1. Specific IBA optimization algorithm flow.

from a fixed value to a dynamic step factor $\alpha(t)$ that changes with the number of iterations. $\alpha(t)$ is defined as follows:

$$\alpha(t) = \frac{t}{T_{\max}} \sinh(1 - \frac{t}{T_{\max}})r \tag{35}$$

where t is the current number of iterations, $T_{\max}$ is the maximum number of iterations, and r is the adjustment coefficient.

The flight mechanism of Levy obeys the Levy distribution, and the mathematical model of the flight mechanism of Levy after variation is as follows:

$$x_i^{t+1} = x_i^t + \alpha(t)\frac{\varphi * \mu}{|\nu|^{\frac{1}{\lambda}}}(x_i^t - x_{best}) \tag{36}$$

where x_{best} is the best bat in the current bat population, $\lambda \in (1, 3)$, φ and μ obey a normal random distribution. The expression of φ is as follows:

$$\varphi = [\frac{\Gamma(1+\lambda) * \sin(\frac{\lambda}{2} * \pi)}{\Gamma(\frac{1+\lambda}{2}) * \lambda * 2^{\frac{\lambda-1}{2}}}]^{\frac{1}{\lambda}} \tag{37}$$

where $\Gamma(x)$ represents the gamma function.

The specific IBA optimization algorithm flow can be obtained by integrating 1) and 2) in section D, as shown in Fig. 1.

As shown in Fig. 1, the IBA introduces a method of dynamically adjusting the search step, which realizes the global search from subspace to the whole solution space by using the proportional relationship between the rate of change of the step factor and the number of iterations. Besides, a larger step can get rid of local extremum. As a result, the original possible search stagnation can be reduced or even disappear. It overcomes the shortcoming of the traditional BA that the global optimization ability is insufficient.

The IBA-optimized SVM model proposed in this section achieves the improvement of reducing the number of convergence and decreasing its complexity on the basis of the original model. Aiming at the characteristics of rolling bearing vibration signal and signal acquisition environment,

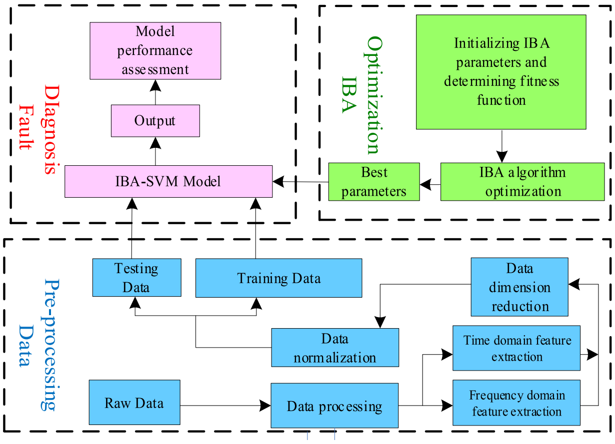

FIGURE 2. Bearing fault diagnosis model based on time-frequency feature extraction and IBA-SVM.

TABLE 1. Fault status information.

Fault type	Fault Diameter (in.)	Number of samples	Category label
	0.007	100	1
Inner Race Fault	0.014	100	2
	0.021	100	3
	0.007	100	4
Outer Race Fault	0.014	100	5
	0.021	100	6
	0.007	100	7
Ball Fault	0.014	100	8
	0.021	100	9
Normal	None	100	10

this IBA-SVM algorithm can accurately and quickly get the diagnosis results, which is suitable for bearing fault diagnosis.

III. BEARING FAULT DIAGNOSIS MODEL BASED ON TIME-FREQUENCY FEATURE EXTRACTION AND IBA-SVM MODEL

In this paper, the time-domain and frequency-domain information of bearing vibration signals are used to extract features, and the IBA algorithm is used to optimize the core parameters of SVM model to improve the accuracy of rolling bearing fault diagnosis. For bearing fault diagnosis, this paper creates a fault diagnosis model, as shown in Fig. 2.

The bearing fault diagnosis model shown in Fig. 2 is mainly composed of data preprocessing, IBA parameter optimization and fault diagnosis. Data preprocessing analyzes and processes the original data samples, including data processing, feature extraction, data dimension reduction, and data normalization, etc. The feature extraction includes two parts: time domain feature extraction and frequency domain feature extraction. IBA parameter optimization uses IBA group intelligent algorithm to optimize parameters in the solution space. The optimal parameters of the model are obtained. Fault diagnosis uses the training set of data samples to train the model, to detect the fault of the divided test set, to analyze the diagnosis results, and to evaluate the performance of the model.

IV. CASE ANALYSIS

A. DATA SOURCE AND ANALYSIS

The data samples used in this research came from the bearing data of Case Western Reserve University, United States. The disclosed bearing data set comprises four states, namely a normal state, an outer face fault, an inner face fault and a rolling ball fault. Except the normal state, the other three states all contain data of three different fault degrees, and there are ten state data in total. The fault status information used in the experiment is shown in Table 1. The sampling frequency of the driving end is 48 kHz, the load is 0 HP. Select the data in the no-load state cause when the bearing fails, we generally do not let the bearing continue to run, prevent secondary mechanical failure, we generally take off the bearing to analyze the fault type of the bearing, when the bearing runs again, it is empty, and the fault type of the bearing can be safely identified. Second, there are many load types of bearings, and different load types and sizes can generate different signals under the same fault. Experiments under no-load conditions can avoid many signal interference and make the diagnosis more accurate. And 100 samples are taken for each type of data, and 1000 samples are obtained in total.

In the analysis, 2500 sample points of inner ring fault, outer ring fault, rolling element fault and normal state with the fault diameter of 0.007 inch are selected, and the waveforms in time-domain under various states can be obtained after simple processing, as shown in Fig. 3.

As can be seen from Fig. 3, the difference between the various states is not sharp enough. If the classification only relies on a feature, satisfactory results cannot be achieved; if all the feature data in the original data set are used to classify the fault, the running speed of the model will inevitably be affected, and the classification accuracy is low, leading to poor diagnosis effect. Thus, prior to model training, the original sample data needs to be preprocessed.

B. DATA PRE-PROCESSING

The data preprocessing of rolling bearing vibration signal mainly includes feature extraction, data dimension reduction and data normalization.

1) FEATURE EXTRACTION

Because the diagnosis effect is not ideal by directly using the signal in the time domain for fault classification, the feature extraction is carried out by integrating

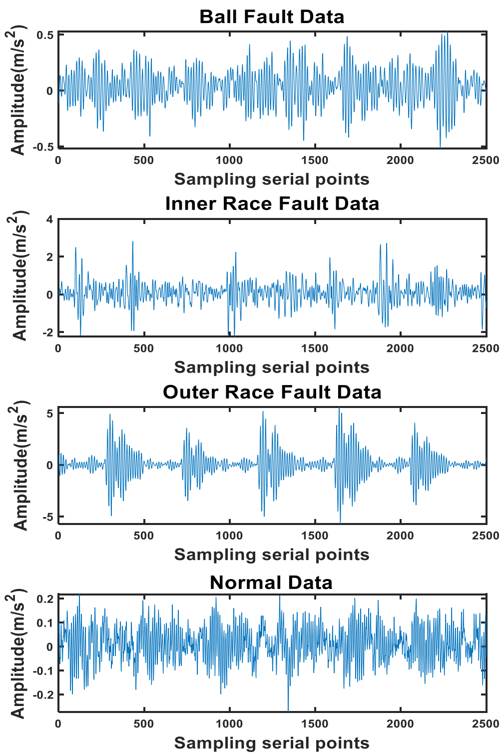

FIGURE 3. Time-domain waveform of bearing vibration signal in four States.

the time-domain feature and frequency-domain feature in this paper. The time-domain feature is mainly some characteristic parameters of the time-domain signal, and the frequency-domain feature is the spectrum signal after FFT processing.

As the simplest and most direct signal analysis method, time domain analysis is currently used in most on-line monitoring systems of rolling bearings. In general, it analyzes signals by calculating simple statistical features of signals, and then selects appropriate characteristic parameters to accurately classify different types of faults. Statistical parameters are divided into two categories based on the existence or absence of dimensions.

The first category is dimensional statistical parameters, namely dimensional statistical parameters, including maximum value, minimum value, variance, mean value, square root magnitude and average amplitude. The other is dimensionless statistical parameters, including kurtosis, skewness, margin index, waveform index, impulse index, peak value index and root mean square value.

According to the different working conditions, a dimensional characteristic value of the size of the corresponding change, and the work environment has a great influence on dimensional characteristic value, has the defect of performance is not stable, bring certain difficulty to engineering application, and the dimensionless index is not sensitive to the change of load and rotating speed, can appear to be more intuitive rotating equipment running status information. Therefore, dimensional characteristic indicators are often used together with dimensionless indicators.

Using dimensional statistical parameters to describe the bearing state can reflect part of the fault information. Dimensional eigenvalues are easy to understand and calculate, so they are often used by researchers. The mean value of the signal cannot reflect the dynamic change of the sample data and is usually used for detection, but the mean value is usually used for calculation of other parameters. In engineering applications, the root mean square value, absolute mean value and root amplitude will increase as the health state of the equipment changes until it fails completely.

The peak value index in the dimensionless eigenvalue reflects the peak-peak degree in the waveform. The impulse index is the signal peak divided by the average value of the absolute value of the signal; Similar to the peak value index, the impulse index can also represent whether there is an instantaneous peak in the vibration signal. Kurtosis index can describe the distribution of variables well. The margin index can usually represent the fatigue wear degree of the component. In practical engineering application, when the sample data is multiplied, the dimensionless features remain unchanged, but the dimensionless features become larger. In the early stage of the equipment health status change, there are many small peaks, which can detect that the root mean square value does not change much. However, due to the high sensitivity of margin index, kurtosis index and pulse index to the pulse-to-health status change, the above three indicators will rise first and then fall. The results showed that the root mean square value was stable, but the sensitivity to the change of health state was low. The stability of index, kurtosis index and pulse index is worse than the root mean square value, but it can better represent the information of health status change of equipment in the early stage.

For ensuring the accuracy of feature selection, the time-domain features extracted in this paper include dimensional feature parameters and dimensionless feature parameters. In total, 13 features are extracted as partial feature inputs. The time-domain characteristic values of the four states in Fig. 2 are shown in Table 2.

There are many data analysis methods in time-frequency domain, such as Wavelet Transform (WT) and Short Time Fourier Transform (STFT), but both of them have their own limitations. WT method needs to select appropriate basis functions; SIFT method requires a suitable window function to determine its resolution. Therefore, the time and frequency resolution cannot be optimized simultaneously [31], [32], [33]. FFT has the characteristics of fast processing speed, no need to set predefined parameters and strong frequency resolution, so FFT is used to process the time-domain bearing vibration signal in this paper.

The time-domain vibration signal of the rolling bearing is sampled by the processor and is a discrete signal, and the frequency spectrum function can be obtained by FFT:

Appropriate sample length needs to consider two problems: (1) too large dimension of a single sample will increase

TABLE 2. Characteristic values of bearing vibration signals in time domain of four states.

	Ball fault	Inner race fault	Outer race fault	Normal	Unit
Maximum value	0.5265	2.8262	5.5885	0.2178	m/s^2
Minimum value	-0.5169	-2.2361	-5.7104	-0.2729	m/s^2
Variance	0.0232	0.3273	1.4462	0.0052	$(m/s^2)^2$
Mean value	0.0329	0.0851	0.0138	0.0123	m/s^2
Square root magnitude	0.1048	0.3370	0.5295	0.0500	m/s^2
Average amplitude	0.1238	0.4172	0.7486	0.0588	m/s^2
Kurtosis	0.0019	0.6652	14.4495	8.0296e-05	None
Margin index	5.0227	8.3857	10.7727	5.4588	None
Waveform indicator	1.2596	1.3861	1.6063	1.2439	None
Pulse indicator	16.0094	33.2120	414.6191	22.2234	None
Skewness	0.0020	0.1120	0.1372	1.5658e-04	None
Peak indicator	0.5265	2.8262	5.7041	0.2729	None
Root mean square	0.1559	0.5783	1.2024	0.0732	None

the calculation and storage load of the computer; (2) the vibration acceleration signal represents the instantaneous change of physical quantity, and too long single sample will reduce the sensitivity of the diagnosis model. Therefore, it is necessary to reasonably select the sample length and preserve the data features as much as possible.

Because FFT extracts the period on the basis of the sampling frequency, the extracted hidden period can represent the period of the whole signal sequence to a certain extent, so it is chosen as the basis for dividing the sample length.

Based on the above analysis, in this paper, the sampling frequency is set to 48000 Hz, the starting point of the sample is randomly selected, and the length of each sample is 864. This length includes two fault cycles, which does not reduce the accuracy due to too long length, but also retains most of the data features. Fig.4 shows the frequency spectra of the four vibration time-domain signals in Fig. 3 after FFT processing.

It can be seen from Eq. (1) and Fig. 4 that when the value of the sample length N changes, a sharp spectral peak will appear in the spectrogram with the fluctuation of the amplitude, the sharpest spectral peak corresponds to a frequency, and the reciprocal of this frequency is the hidden period of the signal.

Because the essence of feature extraction is to preserve the original data information as much as possible and reduce the complexity. The FFT can obtain the distribution of the frequency components of the signal in the spectrogram, and can provide more intuitive information content than the time domain waveform. Unlike most literatures, we do not extract spectrum features like time domain features. Therefore, on the premise of preserving frequency domain information as much as possible, this paper chooses the frequency spectrum obtained by FFT transformation as the frequency domain feature input directly.

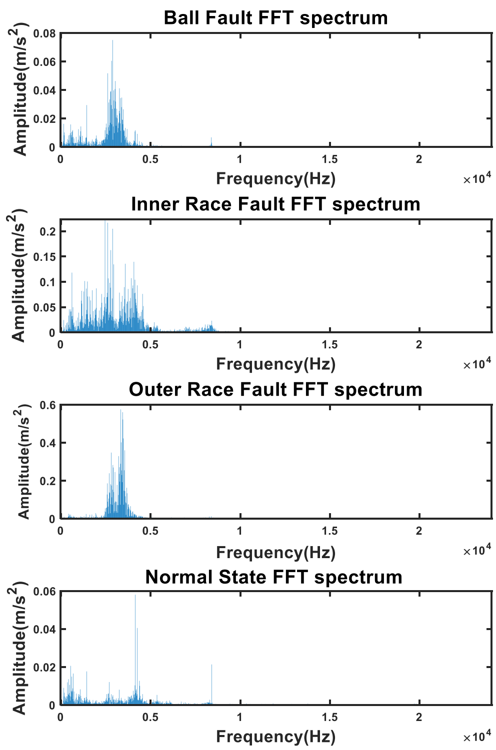

FIGURE 4. FFT spectra of the four-state sampling point.

The 433-dimensional feature data obtained by the FFT are combined with the 13-dimensional time-domain feature data to serve as the input feature data of the IBA-SVM model.

2) DATA DIMENSION REDUCTION

The data set used in this paper has a large amount of data. There are 10 types of data, each type of data has 100 samples, and the matrix dimension of each sample after feature extraction reaches 446 dimensions. If the extracted feature

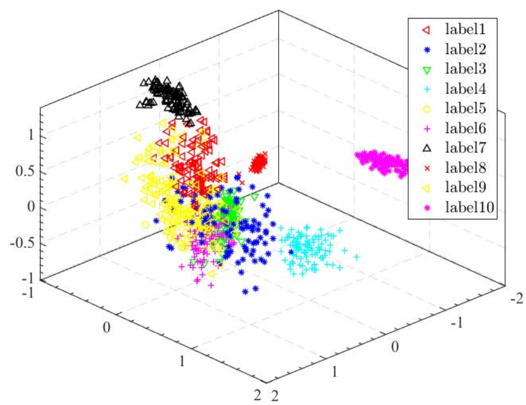

FIGURE 5. **Dimensionality reduction results of feature data.**

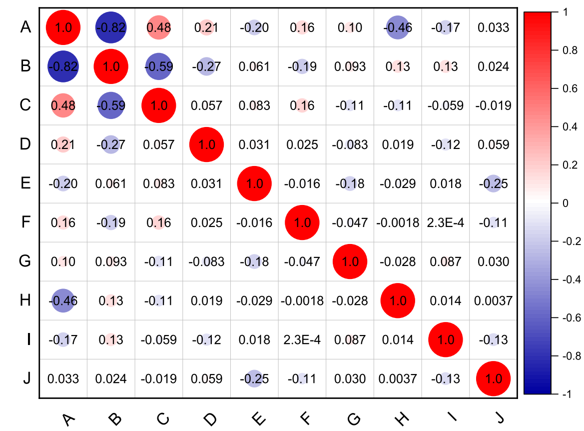

FIGURE 6. **Spearman correlation coefficient diagram of dimensionality reduction data.**

data are directly used to train the model, the dimension is too large, resulting in data redundancy and overfitting. Therefore, it is necessary to reduce the dimensionality of the extracted feature data before normalization to improve the diagnosis performance of the model [31].

MDS is a commonly-used nonlinear dimensionality reduction method that can keep the distance of samples in the original space unchanged in the lower dimensional space, and preserve the relative relationship of data in the original space [29]. Compared with the linear dimensionality reduction methods such as Principal Component Analysis (PCA) and Linear Discriminant Analysis (LDA) [34], [35], MDS algorithm has the advantages of no prior knowledge, simple calculation and good data visualization effect. So, this paper chooses MDS algorithm to reduce the dimensionality of data.

In this paper, the MDS algorithm is used to reduce the feature data to 10 dimensions, with the dimensionality reduction results of 10 types of samples shown in Fig. 5.

It can be seen from Fig. 5 that the selected ten kinds of state data of inner ring fault, outer ring fault, rolling body fault and normal state have excellent discrimination effect after MDS processing, which proves the effectiveness of MDS in dimensionality reduction. The 10 kinds of label samples have high discrimination in space, and the data after MDS-based dimensionality reduction have more recognition and are beneficial for model classification. Besides, it is beneficial to improving the diagnosis efficiency and accuracy of the model.

In order to characterize the correlation between dimensionality reduction features, Spearman correlation coefficient is used to test the correlation between features.

For variables x_i and y_i, Spearman correlation coefficient is calculated by:

$$\rho = 1 - \frac{6\sum_{i=1}^{n}(R_i - Q_i)}{n(n^2-1)} \tag{38}$$

where, R_i represents the rank of x_i, Q_i represents the rank of y_i, $R_i - Q_i$ is the difference of the rank of variable x_i, y_i, and n represents the number of samples. And Spearman correlation coefficient diagram is shown in the Fig. 6.

In Fig. 6, A to J in the horizontal and vertical axes represent the 10-dimensional optimal feature subset described above in turn. According to the definition of Spearman's correlation coefficient, the absolute value of the correlation coefficient is close to 1, which means the higher the correlation is, while 0 means there is no correlation. For classification problems, the lower the correlation, the greater the difference between features, that is, the more favorable the final classification result. As can be seen from Figure 5, the correlation of the 10-dimensional feature subset obtained by MDS dimensionality reduction is low, which is more conducive to the accurate prediction of the model.

3) DATA NORMALIZATION

In this paper, the interval value method is used to normalize the data, so that the data can be scaled to a specific interval to avoid the interaction between the values. Here, the extreme value method is selected for linear function transformation:

$$X_i' = \frac{X_i - \min X_i}{\max X_i - \min X_i} \tag{39}$$

$$X_i'' = X_i' * (mx - mi) + mi \tag{40}$$

where X_i'' is the data after dimension reduction, $(i = 1, 2 \ldots n)$; $\max(x_i)$ is the maximum value in the data sample;$\min(x_i)$ is the minimum value in the data sample; the mapping interval is [-1, 1], default mx is 1, and default mi is -1.

The data after dimension reduction can be used as input for model training and testing after the above normalization processing.

C. BEARING FAULT DIAGNOSIS BASED ON IBA-SVM MODEL

In this paper, K-fold cross-validation is used to optimize the core parameters of the model. The adopted 1000 sample data are divided into a training set and a test set according to a ratio

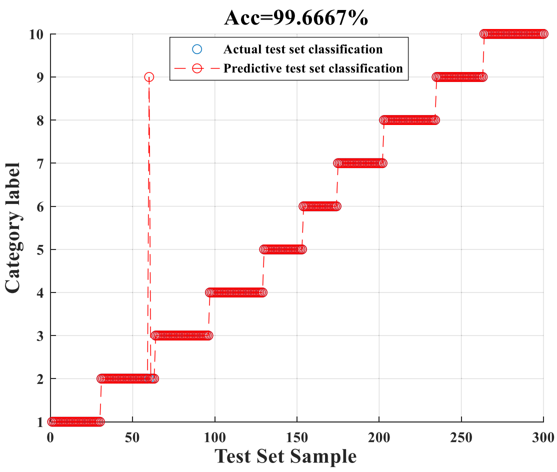

FIGURE 7. Diagnosis result based on time-frequency feature extraction and IBA-SVM.

of 7:3. The K in K-fold cross validation is set to 5, that is, the training set sample is divided into 5 parts, 4 of which are taken as the training set of the five-fold cross validation in turn, and the remaining 1 part is taken as its validation set, so as to find the value of the hyper-parameters that make the model generalization performance optimal. The IBA-SVM model is trained by the training set, and then the trained model is used for fault diagnosis of the test set. The diagnosis result of the IBA-SVM model is shown in Fig. 7.

It can be seen from Fig. 7 that the diagnosis accuracy of the IBA-SVM model is 99.6667%, which has good bearing fault classification effect and excellent diagnosis effect, and has certain practical significance in bearing fault diagnosis.

D. MODEL EVALUATION

In order to verify the superiority of the method proposed in this paper, the following experiments are designed:

Experiment 1 verifies the superiority of SVM model in fault diagnosis.

Deep Extreme Learning Machines (DELM) and Random Forest (RF), BP Neural Network and SVM model were also used for diagnosis as the comparison with the SVM model.

Experiment 2 verifies the superiority of IBA optimization algorithm.

Improved Sparrow algorithm based on Gaussian variation (GSSA), the improved Gray Wolf algorithm based on Difference-mutation (DEGWO), BA and IBA were used to optimize the SVM model to verify the superiority of IBA.

Experiment 3 verifies the superiority of the feature extraction method.

Time-domain features, frequency-domain features and combined time-frequency domain features were used to train and test the model. The results verify the superiority of the time-frequency feature extraction method proposed in this paper.

Experiment 4 verifies the robustness of the model.

Gaussian white noise with different signal to noise ratios was added to the test set to carry out the diagnostic test of the model and test the operation effect of the diagnostic model in the noisy environment.

TABLE 3. Diagnosis results of each algorithm.

Optimization algorithm	c	g	Accuracy (%)	Correct number
GSSA	6.2245	8.7522	92.6667	278
DEGWO	27.5880	0.5538	95.0000	285
BA	28.4414	0.5354	99.3333	298
IBA	37.2536	0.1670	99.6667	299

1) COMPARISON OF MULTI-MODEL DIAGNOSIS RESULTS

In order to verify the superiority of the selected classification model, the preprocessed feature data were put into the DELM, RF, BP neural network and SVM models respectively, and the default parameters were used in the hyperparameters of each model to compare the classification effect of each model. That is, no optimization algorithm is used for parameter optimization. The diagnosis results of each model are shown in Fig. 8.

As can be seen from Fig. 8, the diagnosis effect of the SVM model with default parameters could reach the highest accuracy, with an accuracy rate of 85.3333%, while that of the DELM model is the worst. Therefore, it can be concluded that the SVM model used in this paper has better effect than other models.

2) COMPARISON OF OPTIMIZATION PERFORMANCE OF EACH OPTIMIZATION ALGORITHM

In order to verify the superiority of the above IBA, the optimization algorithm presented in this paper is compared with other advanced algorithms in the field of bearing fault. In this paper, the improved Sparrow algorithm based on Gaussian variation (GSSA), the improved Gray Wolf algorithm based on Difference-mutation (DEGWO), BA algorithm and IBA algorithm are respectively used to optimize the parameters of SVM model. The diagnosis results of each optimization model are shown in Table 3, which contains the parameters C and G optimized by each algorithm, as well as the final classification accuracy and the number of correct classifications.

It can be seen from Table 3 that the diagnosis effect of the classification model is improved after the optimization. The classification effect of each model optimized by the optimization algorithm is obviously improved compared with the original SVM model. The prediction accuracy of IBA-SVM model is higher than that of GSSA -SVM model and DEGWO -SVM model, while the prediction accuracy of BA-SVM and IBA-SVM models is about 99%.

In order to further compare the performance of BA and IBA, the initial population size was set to 20, the number of iterations was set to 200. The best fitness curves of BA and IBA are shown in Fig. 9.

As can be seen from Fig. 9, when the best fitness curve is stable, it means that it has converged. The IBA finds the optimal fitness value when the number of iterations is about

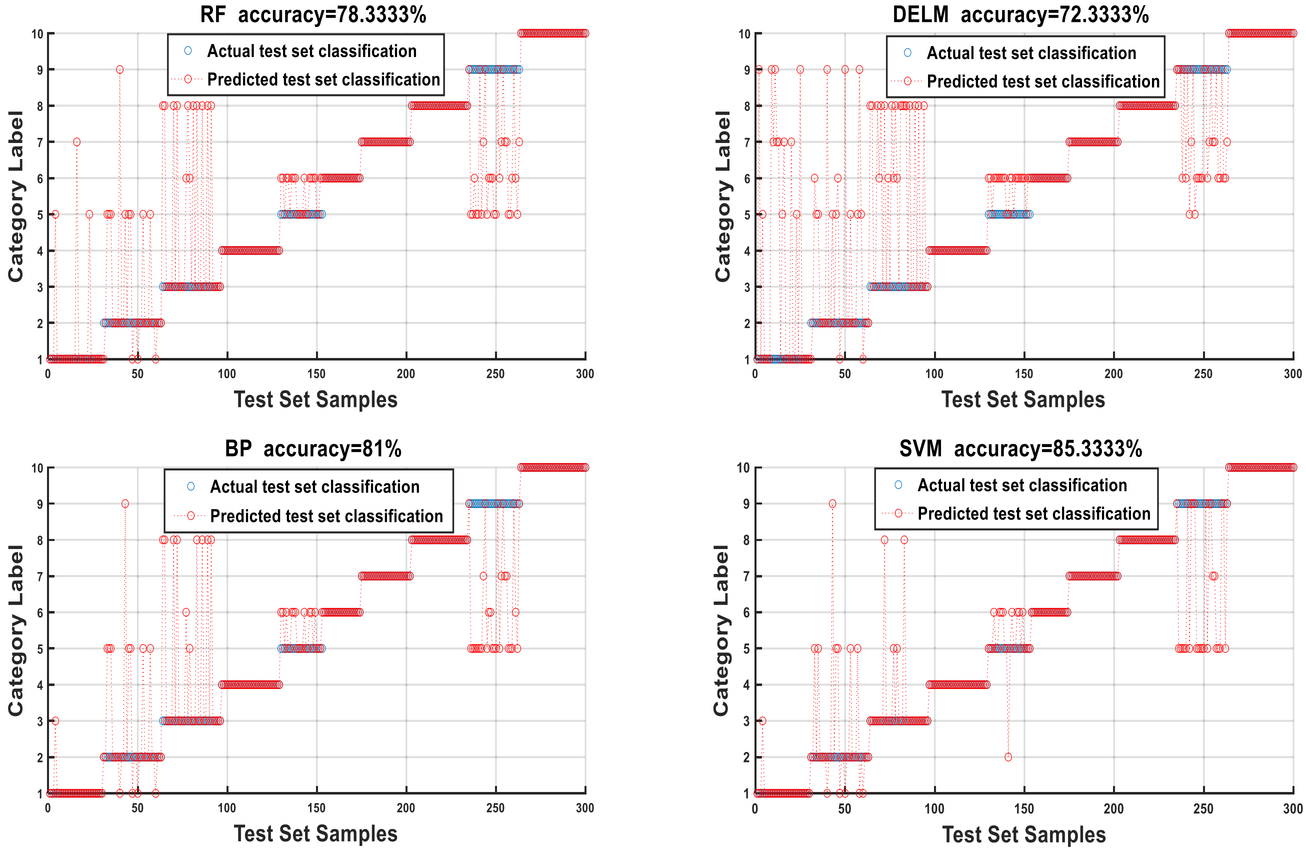

FIGURE 8. Diagnosis results by multiple models.

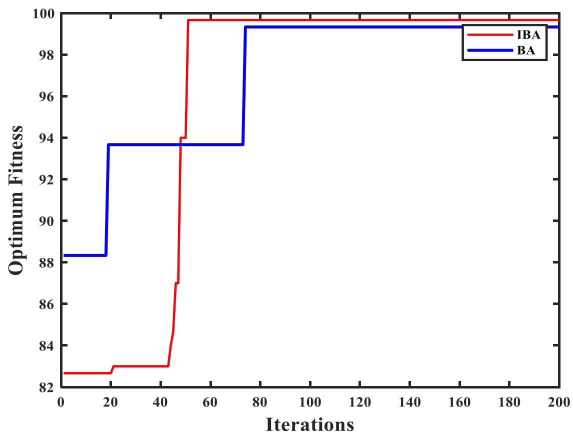

FIGURE 9. Graph of convergence curve.

50, while the BA stays at a certain value in the iteration process, and the convergence speed is slow, and finally converges to the local optimal solution instead of the global optimal solution. Compared with the BA, the IBA has faster iterative convergence speed. It is easy to find the global optimal solution quickly and can overcome the premature phenomenon well. So, the optimization effect of IBA is better than that of BA. IBA-SVM model is 99.6667%, which has good bearing fault classification effect and excellent diagnosis effect, and has certain practical significance in bearing fault diagnosis.

3) COMPARISON OF DIAGNOSIS RESULTS OF DIFFERENT FEATURE EXTRACTION METHODS

In order to verify the superiority of the feature extraction method used in this paper, time-domain features, frequency-domain features and the combined time-frequency domain features were used to train and test the model. Fig. 10 compares the diagnosis results of the IBA-SVM model using the time-domain feature extraction method and the frequency-domain feature extraction method.

By comparing the IBA-SVM model under the time-frequency-domain feature extraction method in Fig. 7, it can be seen that the accuracy of the test set in Fig. 8 is significantly lower than that under the feature extraction method proposed in this paper. It shows that the time-frequency domain feature extraction can obtain better diagnostic results than using time domain or frequency domain features alone. Therefore, the feature extraction method selected in this paper performs better in the test set and has better diagnostic effect.

4) EVALUATION PARAMETERS BASED ON TIME-FREQUENCY FEATURE EXTRACTION AND IBA-SVM MODEL

In order to further verify the superiority of IBA-SVM under time-frequency feature extraction, the macro-average F1 value was used to evaluate the model again. Macro average F1 value is an evaluation index for the comprehensive analysis

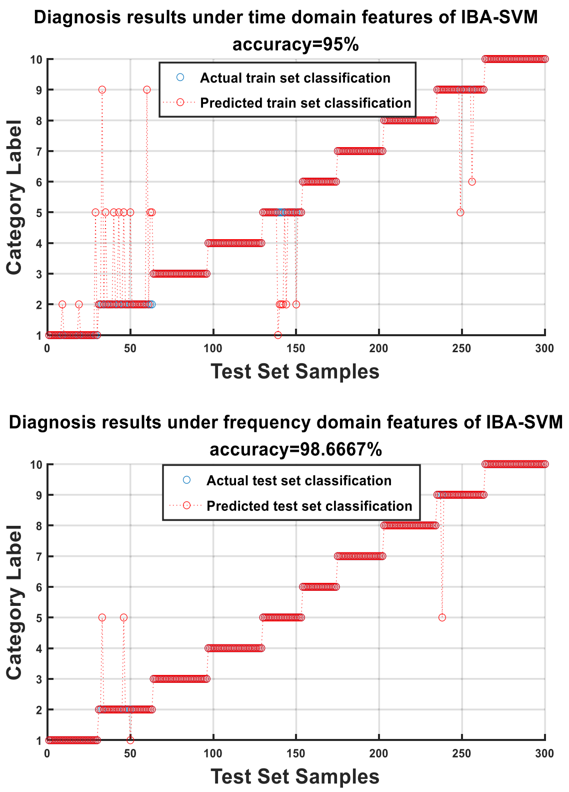

FIGURE 10. Diagnosis results based on time domain feature extraction and frequency domain feature extraction of IBA-SVM model.

TABLE 4. Diagnosis results of IBA-SVM model under time-frequency domain feature extraction method.

Fault label	Test set	TP	FP	FN
Label 1	30	30	0	0
Label 2	33	32	0	1
Label 3	33	33	0	0
Label 4	33	33	0	0
Label 5	24	24	0	0
Label 6	21	21	0	0
Label 7	28	28	0	0
Label 8	32	32	0	0
Label 9	29	29	0	0
Label 10	37	37	1	0
Total	300	299	1	1

of recall and precision, which is the harmonic average of precision and recall, and is also a commonly-used multi-classification evaluation index. The number of all kind of samples in the model diagnosis result was calculated. The results obtained are shown in Table 4.

In Table 4, TP is the positive sample where the prediction is correct, FP is the positive sample where the prediction is wrong, and FN is the negative sample where the prediction is wrong.

The specific values of precision, recall and F1-Score were calculated from Table 4, and the results are shown in Table 5.

TABLE 5. Specific value of each indicator table.

Fault label	Accuracy	Recall rate	F1-Score
Label 1	1	1	1
Label 2	1	0.9697	0.9846
Label 3	1	1	1
Label 4	1	1	1
Label 5	1	1	1
Label 6	1	1	1
Label 7	1	1	1
Label 8	1	1	1
Label 9	0.9667	1	0.9831
Label 10	1	1	1
Average value	0.9967	0.9970	0.9968

Annotation Precision, Recall and F1-Score are calculated by:

$$\Pr ecision = \frac{TP}{TP + FP} \tag{41}$$

$$Recall = \frac{TP}{TP + FN} \tag{42}$$

$$F1 - Score = \frac{2 * P * R}{P + R} \tag{43}$$

where P and R in Eq. (32) represent Precision and Recall, respectively.

The macro average F1 value is the F1 obtained for each fault tag sample. The macro average F1 value based on time-frequency feature extraction and IBA-SVM model is 0.9968. Using the same method, the corresponding values of other models can be obtained respectively, all lower than 0.9968. Therefore, the method selected in this paper has a better classification effect than other methods, and is fully applicable to rolling bearing fault diagnosis.

5) ROBUSTNESS TEST

In order to verify the practicability and anti-interference ability of the proposed diagnosis model based on time-frequency feature extraction and IBA-SVM in the real environment, that is, to verify its robustness. Gaussian white noise with different signal-to-noise ratios (SNR) was based on the test set into the trained IBA-SVM model. Combining the accuracy rate and the macro average F1 value, the performance of the model in the noisy environment was examined.

Here, the Gaussian white noise with the proportions of 1%, 5%, 8%, 10%, 12% and 15% and the corresponding SNRs of 40 dB, 26 dB, 22 dB, 20 dB, 18 dB and 16 dB were selected and added to the test set, and the classification results of the noisy test set are shown in Fig. 11.

It can be seen from Fig. 11 that the model based on time-frequency feature extraction and IBA-SVM proposed in this paper performs well in noisy environments. After adding Gaussian white noise, the accuracy of the model is more than 70%, and the macro average F1 value is more than 0.7. Especially when the SNR is relatively large, such as

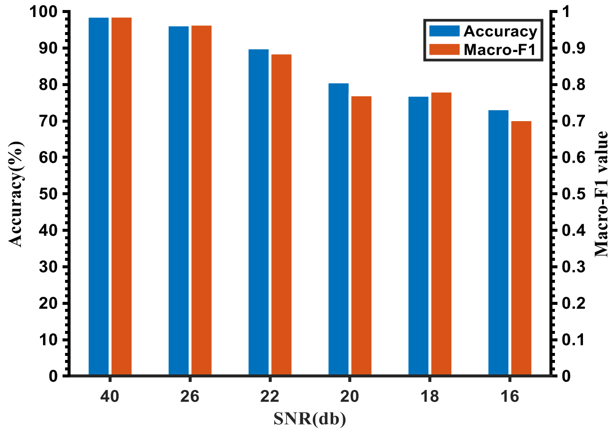

FIGURE 11. Classification results of noisy test set.

SNR = 40 dB, SNR = 26 dB, the operation of the model is almost not affected by noise. This shows that the model has good robustness.

V. CONCLUSION

In order to improve the accuracy of mechanical rolling bearing fault diagnosis, a rolling bearing fault diagnosis method based on time-frequency feature extraction and IBA-SVM algorithm is proposed in this paper. Experiments were conducted to verify the performance of the proposed method. The conclusions are as follows:

(1). The data subjected to time-frequency feature extraction and MDS dimension reduction are more recognizable in the Euclidean space.

(2). Comparison with other classification models shows that the SVM model performs best in the diagnosis results, and the accuracy rate reaches 85.3333%, higher than other models.

(3). Comparison with other optimization algorithms indicates that the IBA has the best hyperparameter optimization effect and the fastest convergence speed in SVM. The IBA-SVM model has the best performance with the accuracy of 99.6667%. Compared with FA-SVM, PSO-SVM and BA-SVM, the accuracy is improved by 12%, 6.3333% and 0.3333% respectively.

(4). The time-frequency feature extraction and IBA-SVM model proposed in this paper performs well in noisy environments with strong anti-interference and robustness.

For rolling bearing fault diagnosis, the case selected in this paper is bearing fault under 0HP. And our future research direction includes the analysis of bearing fault vibration signals under different load conditions and the connection and difference under different load conditions. In addition, most diagnosis methods are currently offline diagnosis, but actually once fault occurs, it will cause a series of negative consequences, such as economic losses, casualties and so on. So we more hope that the online fault diagnosis can be realized, in order to achieve the purpose of real-time detection fault, this will be our future focus in the study of fault diagnosis.

REFERENCES

[1] T. Guiji and W. Xiaolong, "Application of variational modal decomposition method based on parameter optimization to early fault diagnosis of rolling bearing," *J. Xi'an Jiaotong Univ.*, vol. 49, no. 5, p. 9, 2015.

[2] Y. Li, W. Dai, and W. Zhang, "Bearing fault feature selection method based on weighted multidimensional feature fusion," *IEEE Access*, vol. 8, pp. 19008–19025, 2020.

[3] S. Adamczak, K. Stepien, and M. Wrzochal, "Comparative study of measurement systems used to evaluate vibrations of rolling bearings," *Proc. Eng.*, vol. 192, pp. 971–975, Jan. 2017.

[4] Y. Tian, Z. Wang, and C. Lu, "Self-adaptive bearing fault diagnosis based on permutation entropy and manifold-based dynamic time warping," *Mech. Syst. Signal Process.*, vol. 114, pp. 658–673, Jan. 2019.

[5] M. Kang, J. Kim, J.-M. Kim, A. C. C. Tan, E. Y. Kim, and B.-K. Choi, "Reliable fault diagnosis for low-speed bearings using individually trained support vector machines with kernel discriminative feature analysis," *IEEE Trans. Power Electron.*, vol. 30, no. 5, pp. 2786–2797, May 2015.

[6] B. Cai, Z. Wang, H. Zhu, Y. Liu, K. Hao, Z. Yang, Y. Ren, Q. Feng, and Z. Liu, "Artificial intelligence enhanced two-stage hybrid fault prognosis methodology of PMSM," *IEEE Trans. Ind. Informat.*, vol. 18, no. 10, pp. 7262–7273, Oct. 2022.

[7] X. Kong, B. Cai, Y. Liu, H. Zhu, Y. Liu, H. Shao, C. Yang, H. Li, and T. Mo, "Optimal sensor placement methodology of hydraulic control system for fault diagnosis," *Mech. Syst. Signal Process.*, vol. 174, Jul. 2022, Art. no. 109069.

[8] X. Han, Z. Wang, M. Xie, Y. He, Y. Li, and W. Wang, "Remaining useful life prediction and predictive maintenance strategies for multi-state manufacturing systems considering functional dependence," *Rel. Eng. Syst. Saf.*, vol. 210, Jun. 2021, Art. no. 107560.

[9] Z. Liu, W. Guo, J. Hu, and W. Ma, "A hybrid intelligent multi-fault detection method for rotating machinery based on RSGWPT, KPCA and twin SVM," *ISA Trans.*, vol. 66, pp. 249–261, Jan. 2017.

[10] Y. Yang, Y. Liao, G. Meng, and J. Lee, "A hybrid feature selection scheme for unsupervised learning and its application in bearing fault diagnosis," *Expert Syst. Appl.*, vol. 38, no. 9, pp. 11311–11320, Sep. 2011.

[11] M. S. Ballal, Z. J. Khan, H. M. Suryawanshi, and R. L. Sonolikar, "Adaptive neural fuzzy inference system for the detection of inter-turn insulation and bearing wear faults in induction motor," *IEEE Trans. Ind. Electron.*, vol. 54, no. 1, pp. 250–258, Feb. 2007.

[12] S. Gao, L. Xu, Y. Zhang, and Z. Pei, "Rolling bearing fault diagnosis based on SSA optimized self-adaptive DBN," *ISA Trans.*, Dec. 2021, doi: 10.1016/j.isatra.2021.11.024.

[13] Q. Aisong, L. Yunrong, Z. Qinghua, H. Qin, and S. Guoxi, "Fault classification of rolling bearing based on extreme learning machine optimized by bat algorithm," *Comput. Meas. Control*, vol. 27, no. 5, p. 5, 2019.

[14] S. Liye and S. Lin, "Research on rolling bearing fault diagnosis based on EEMD-GSSA-SVM," *Sensors Microsyst.* vol. 41, no. 4, pp. 56–59, 2022, doi: 10.13873/J.1000-9787(2022)04-0056-04.

[15] L. Qian, Z. Wang, and Z. Zhou, "Rolling bearing fault diagnosis method based on SSA-ELM," in *Advanced Intelligent Technologies for Industry*. Singapore: Springer, 2022, pp. 531–538.

[16] X. Xiaoting, L. Shaobo, and Y. Guanchi, "Based on fault diagnosis of rolling bearing based on FFT and CS-SVM," *Modular Mach. Tool Autom. Machining Technol.*, vol. 205, no. 4, pp. 90–94, 2019, doi: 10.13462/j.cnki.mmtamt.2019.04.022.

[17] Z. Xingtong, "Bearing fault diagnosis method based on bat algorithm optimized relevance vector machine," *Automat. Instrum.*, vol. 2, pp. 21–24, Jan. 2021, doi: 10.14016/j.cnki.1001-9227.2021.02.021.

[18] F. Yufang, L. Houqing, and Y. Hong, "Based on research on fault diagnosis model based on BP neural network," *Comput. Eng. Appl.*, vol. 55, no. 6, p. 7, 2019.

[19] L. Qiang and C. Wenlong, "Motor fault diagnosis based on improved particle swarm optimization neural network," *Electr. Drive*, vol. 50, no. 1, pp. 103-108, 2020, doi: 10.19457/j.1001-2095.dqcd19090.

[20] M. Zhang, W. Chen, Y. Zhang, F. Liu, D. Yu, C. Zhang, and L. Gao, "Fault diagnosis of oil-immersed power transformer based on difference-mutation brain storm optimized catboost model," *IEEE Access*, vol. 9, pp. 168767–168782, 2021.

[21] G. Xiaoping, Y. Ruichen, and L. Yuan, "Based on multi-type fault diagnosis of MDP-SVM process," *Electron. Meas. Technol.*, vol. 45, no. 1, pp. 159–164, 2022, doi: 10.19651/j.cnki.emt.2107999.

[22] Z. Jin, D. He, Y. Chen, C. Liu, and S. Shan, "Research on fault diagnosis method of train rolling bearing based on variational modal decomposition and bat algorithm-support vector machine," *J. Phys., Conf. Ser.*, vol. 1820, no. 1, Mar. 2021, Art. no. 012170.

[23] Y. Qin, L. Jin, A. Zhang, and B. He, "Rolling bearing fault diagnosis with adaptive harmonic kurtosis and improved bat algorithm," *IEEE Trans. Instrum. Meas.*, vol. 70, pp. 1–12, 2021, doi: 10.1109/TIM.2020.3046913.

[24] B. Wang, Y. Lei, N. Li, and N. Li, "A hybrid prognostics approach for estimating remaining useful life of rolling element bearings," *IEEE Trans. Rel.*, vol. 69, no. 1, pp. 401–412, Mar. 2020.

[25] W. A. Smith and R. B. Randall, "Rolling element bearing diagnostics using the case western reserve university data: A benchmark study," *Mech. Syst. Signal Process.*, vol. 64, pp. 100–131, Dec. 2015.

[26] L. Cheng, "Novel metaheuristic bat algorithm," *Comput. Knowl. Technol.*, vol. 2010, no. 23, p. 4, 2010.

[27] J. Weijian and W. Chunzhi, "Research on cloud computing resource allocation based on bat algorithm," *Comput. Appl. Res.*, vol. 32, no. 4, p. 4, 2015.

[28] L. Zhen, H. Zhengjia, Z. Yanyang, and C. Xuefeng, "Bearing condition monitoring based on shock pulse method and improved redundant lifting scheme," *Math. Comput. Simul.*, vol. 79, pp. 318–338, Dec. 2008, doi: 10.1016/j.matcom.2007.12.004.

[29] L. Changping and Y. Chunming, "Have the bat algorithm for flight characteristics of Lévy," *J. Intell. Syst.*, vol. 10, no. 3, pp. 240–246, 2013.

[30] Y. Wenzhen, H. Qing, and D. Ruisuo, "Locust optimization algorithm with perturbation mechanism and enhanced Lévy flight," *Mini-Microcomput. Syst.*, vol. 43, no. 2, p. 7, 2022.

[31] Y. Wenzhe, X. Hong, and P. Binsen, "Based on fault diagnosis method of rolling bearing based on FFT and CNN," *Appl. Technol.*, vol. 48, no. 6, p. 5, 2021.

[32] W. Sun, G. An Yang, Q. Chen, A. Palazoglu, and K. Feng, "Fault diagnosis of rolling bearing based on wavelet transform and envelope spectrum correlation," *J. Vib. Control*, vol. 19, no. 6, pp. 924–941, Apr. 2013.

[33] J. B. Ali, L. Saidi, A. Mouelhi, B. Chebel-Morello, and F. Fnaiech, "Linear feature selection and classification using PNN and SFAM neural networks for a nearly online diagnosis of bearing naturally progressing degradations," *Eng. Appl. Artif. Intell.*, vol. 42, pp. 67–81, Jun. 2015.

[34] P. Liran, J. Pingping, and Y. Guozheng, "Research on fall detection algorithm based on support vector machine," *Opticalnprecision Eng.*, vol. 25, no. 1, pp. 182–187, 2017.

[35] C. Y. Yang and T. Y. Wu, "Diagnostics of gear deterioration using EEMD approach and PCA process," *Measurement*, vol. 61, pp. 75–87, Feb. 2015.

MEI ZHANG was born in Suzhou, Anhui, China, in 1979. She received the bachelor's and master's degrees in electrical engineering from the Anhui University of Science and Technology, in 2002 and 2005, respectively. She is currently an Associate Professor with the School of Electrical and Information Engineering, Anhui University of Science and Technology. Her research interests include intelligent control, the Internet of Things (IoT) technology, and embedded systems.

JUN YIN was born in Xuancheng, Anhui, China, in 1998. He received the bachelor's degree in electrical engineering and automation from the Anhui University of Science and Technology, where he is currently pursuing the M.E. degree in energy dynamics. His research interests include fault diagnosis and intelligent detection.

WANLI CHEN was born in Taizhou, Zhejiang, China, in 1996. He received the bachelor's degree in electrical engineering from the Xinjiang Institute of Technology, in 2020. He is currently pursuing the master's degree with the Anhui University of Science and Technology. His research interests include intelligent control Internet of Things technology, the Internet of Things (IoT) technology, and data analysis.